



Flux Regulation of Induction Motor at Low Speed using Direct Torque Control

Anjuna S. Babu¹, Shahina T.N²
M.Tech Student¹, Assistant Professor²
Department of Electrical and Electronics
TKMCE, Kollam, Kerala, India

Abstract:

This paper presents a Constant Switching Frequency Controller (CSFC) for improving stator flux regulation at very low speed regions in a DTC-lookup table based Induction motor. The stator flux regulation is improved under no load by replacing the hysteresis torque comparator with CSFC without any change to the look-up table. Hence the simple structure of DTC is maintained in this method. The flux droop problem that normally occurs on hysteresis based DTC is resolved using DTC-CSFC as well as constant switching frequency is maintained at low speed. In order to reduce the torque ripples, and hence improve the estimation process at very low speed, Extended Kalman Filter (EKF) is used in this work.

Keywords: Direct torque control; Constant Switching Frequency Controller; flux regulation; induction motor; extended kalman filter.

I. INTRODUCTION

Induction motors especially squirrel cage induction machine, are relatively rugged, has very compact structure and cheap machines. Also, it does not require periodic maintenance like DC motors. Therefore much attention must be given to their control for various applications with different control methods. In the past two decades, field oriented control (FOC) method is the most popular induction motor drive control method. FOC method uses sensor less techniques that avoid the use of speed sensor and flux sensor. These sensors are replaced with state observers to minimize the cost and increase the reliability in hardware. In the middle of 1980's, Direct Torque Control (DTC) of induction motor (IM) proposed by Takahashi has started to gain popularity in advanced industrial applications due to the advantages of its simple configuration and quick dynamic response robustness. The DTC can provide good torque control with simpler structure, and does not require knowledge of complex field orientation block, speed encoder, machine parameters and current regulation loop; this is the main advantage of DTC over Field Oriented Control (FOC) method. The basic concept of DTC utilizing hysteresis torque controller, which is referred to as DTC-HC, is that, it is based on a three-level torque comparator, a two-level flux comparator, to select voltage vectors and a stator flux position from a predefined switching table. After the introduction of DTC-HC several variations to its original structure were proposed to overcome its drawbacks in hysteresis-based controller such as poor flux regulation at low speed, high torque ripple, and high sampling frequency requirement for digital implementation. DTC drives are inherently sensor-less, but for low speed operations and speed control, the rotor speed information is still needed. In order to increase the reliability of adjustable speed drive systems reduce the cost for estimating the speed based on the terminal variables instead of using the mechanical sensors has becoming one of the most important research areas. The flux droop problem (i.e., poor stator flux regulation at low speed operation), high torque ripples, and variable switching frequency are the major

problems in DTC involving hysteresis torque controller. The high torque ripples, and variable switching frequency can be controlled by space vector modulation, known as the DTC-SVM. Using this method, hysteresis comparators are not needed for the flux and torque control. The main disadvantage of DTC-SVM is that they require extensive computation and the stability at very low and zero speed. The switching frequency becomes unpredictable when we adjust the torque error and flux within the fixed hysteresis bands. To avoid this problem, here we use constant switching frequency controller (CSFC) instead of the torque comparator of DTC-HC. In this paper, we also study the performance of DTC-CSFC near and at zero frequency. With DTC-CSFC, flux regulation can be achieved at zero and low frequency, which is the condition for any speed observer to work effectively. Here we also use an Extended Kalman Filter (EKF), for speed estimation which has high convergence rate and good disturbance rejection, and will not be affected by unmeasured disturbances. There are two types of EKF techniques employed for speed sensorless IM drives: reduced order and full order estimators. For systems with complex control structure systems that require high computational requirement, we don't demand much on the reduced order EKF. Another disadvantage of reduced order EKF is that it reduces the accuracy and reliability of estimated states. To improve the sensitivity against parameter variation, we use two switching EKFs with seventh order. To establish flux coupling between rotor and stator and enhance IM drives at low and zero speeds, we use the equation of motion, for sixth order system. In order to improve EKF performance under different noise conditions, we use Multi-EKFs. On comparing the above EKF's the common disadvantage is its heavy computational requirements compared to the normal EKF. In this paper, CSFC is used by replacing the hysteresis torque controller without increasing the complexity of the control structure. So, the conventional EKF algorithm combined with DTC-CSFC is used to improve performance at low and zero speed regions, with smaller sampling period, and hence achieving larger control bandwidth. The performance of the proposed EKF estimator is

good and acceptable, due to the improved stator flux regulation. Also, EKF-based DTC-CSFC will reduce the torque ripple as well as increase the dynamic performance for step changes of speed from different low speed regions. In the following section, principle of DTC is described. In section III, flux regulation of basic DTC at low speed is briefly described. Section IV describes the improvement of flux regulation of DTC using CSFC. The extended IM model and the discrete form of EKF algorithm is presented in Section V. Finally, the conclusion is presented in Section VI.

II. DIRECT TORQUE CONTROL

After the development of Vector Control scheme, direct torque control (DTC) method was developed which has high performance technology. The main advantage of using DTC method is its ability to control the torque and the flux without using the (d-q) park coordinates in a closed-loop manner without using current loops; (ie, Coordinate transformation is not required). The current is not regulated directly, so current control loops are not required. It calculates the instantaneous values of flux and torque in the induction machine. The reference flux ψ_s^* and torque T_e^* are compared with the calculated values of torque and flux. DTC scheme can only be applied to power electronic converter-fed machines, since it uses simple processing method and depends fully on the non-ideal nature of the power source. The DTC induction motor drive is supplied by a voltage source inverter (VSI), in order to control directly the stator flux linkage and electromagnetic torque by the selecting optimal inverter switching modes. The selection of flux and torque hysteresis bands is done such as to get fast torque response, low inverter switching frequency, and low harmonic losses.

The control system of DTC consists of a torque controller, PI torque controller, the polar-to-rectangular transformation of direct stator flux control and a stator voltage calculation blocks, and the stator flux and torque estimation block. The reference torque T_e^* is obtained from the output of the PI speed controller; and is compared with the estimated torque T_e to generate an error signal; this is shown in Fig. 1. Here the stator flux is controlled by hysteresis controller which has two levels for limiting the variation of the flux module within its reference value and the electromagnetic torque is controlled by hysteresis controller which has three levels in order to develop the desired torque and controlling the machine in both directions of rotation. So the and control and estimation of these variables becomes simple.

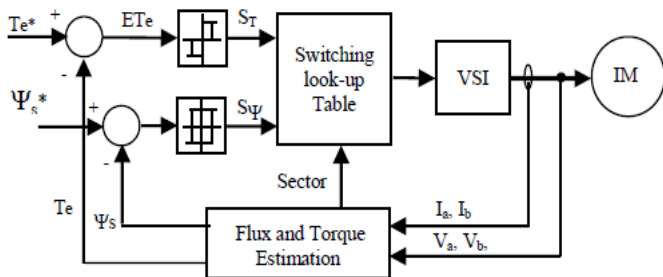


Figure.1. Structure of DTC of Induction motor.

The structure of DTC is shown in Fig. 1. It consist of a pair of hysteresis comparator, switching table, 3-phase voltage source inverter (VSI) and, torque and flux estimators. The main

disadvantages of using DTC with PI controllers are variable switching frequency, high ripples in current and torque and low operating conditions.

III. FLUX REGULATION OF BASIC DTC AT LOW SPEED

Due to increasing popularity DTC has become and is considered as an alternative controller for FOC. There are three types of current controllers, namely; ramp-comparator-based controllers, hysteresis controllers, and predictive controllers [11]. The initially proposed structure of DTC-HC is shown in Fig. 2. There is a predetermined switching table (look-up table), which determines the stator flux position and whether the torque and the stator flux need to be increased or decreased. Based on the selection of the switching states (S_a, S_b, S_c) which is obtained from a predetermined switching table, the output stator voltage is applied.

By selecting suitable voltage vectors, the stator flux space vector as well as electromagnetic torque can be simultaneously controlled, in DTC. The DTC of induction machine drive can exploit under over modulation mode by controlling the locus of stator flux.

Depending on the torque and stator flux demands, the selection of suitable voltage vectors from the look-up table. The rule is as shown in Table I. The rate of change of stator flux vector is obtained from the stator voltage equation of IM is given by (1).

$$\frac{d\psi_s}{dt} = v_s - i_s R_s \quad (1)$$

Where Ψ_s, \mathcal{G}_s and i_s are the stator flux linkage, stator voltage, and stator current space vectors respectively. R_s is the stator resistance. For a very short duration of time, (1) can be written as:

$$\Delta\psi_s = (v_s - i_s R_s) \Delta t \quad (2)$$

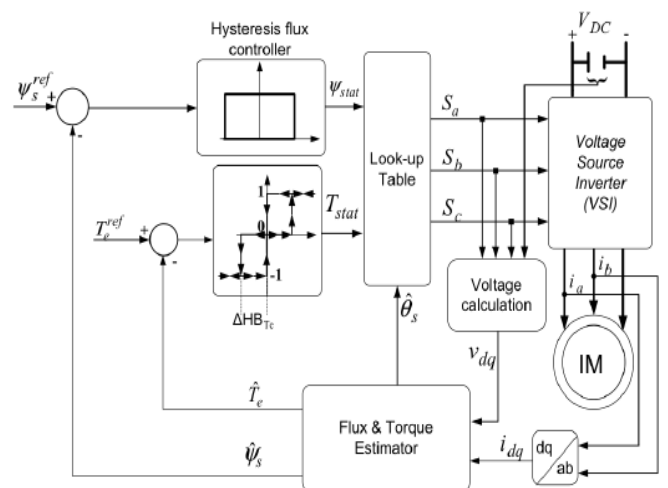


Figure. 2. Basic DTC-HC structure.

When controlling the flux in DTC of IM is based on (2), since we neglect the stator resistance drop when selecting voltage vectors from the look-up table. Therefore (2) can be approximated by (3):

$$\Delta\psi_s \approx \mathcal{G}_s (\Delta t) \quad (3)$$

Table. I. Selection of voltage vectors

		<i>Voltage vector selections</i>	
Flux need to be increased	Torque need to be reduced	Zero voltage vector (A)	Reverse active voltage vectors
	Torque need to be increased	Forward active voltage vectors	
Flux need to be increased	Torque need to be reduced	Zero voltage vector (A)	Reverse active voltage vectors
	Torque need to be increased	Forward active voltage vectors	

To reduce the torque (labeled as (A) and (B) in Table I) is based on (3); it is assumed that the stator flux freezes ($\Delta\psi_s = 0$) when zero voltage vectors are selected. When the ohmic drop in (1) is considered, selection of a zero voltage vector resulted in a reduction in stator flux, as given by (4):

$$\Delta\psi_s = -i_s R_s (\Delta t) \tag{4}$$

The change in stator flux in (4) is negligibly small, since the duration Δt is small and also when the motor current is small (ie; light load). The duration Δt depends on how long the torque waveform take to travel from upper to the lower band as shown by Fig. 4. Let the duration taken by torque to travel from lower band to the upper band (positive torque slope) and from upper band to the lower band (negative torque slope) be Δt_1 and Δt_2 respectively. From the figure it can be seen that in order for the flux to have a net positive increment, hence proper flux regulation,

$$\Delta\psi_{s1} > \Delta\psi_{s2} \tag{5}$$

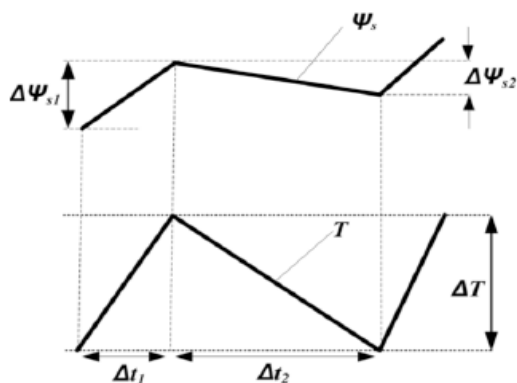


Figure. 4. Stator flux and torque waveform.

Note that $\Delta\psi_{s1}$ is represented by (2) and $\Delta\psi_{s2}$ is represented by (4). Therefore we can write:

$$|(\vartheta_s - i_s R_s) \Delta t_1| > |s R_s| \Delta t_2 \tag{6}$$

Since $\frac{\Delta T}{\Delta t_1} = \text{positive } T \text{ slope}$ and $\frac{\Delta T}{\Delta t_2} = \text{negative } T \text{ slope}$, so

we can write (5), which is the condition needed for flux regulation, as

$$\frac{\Delta t_1}{\Delta t_2} = \frac{\langle \text{negative } T \text{ slope} \rangle}{\langle \text{positive } T \text{ slope} \rangle} > \frac{|i_s R_s|}{|(\vartheta_s - i_s R_s)|} \tag{7}$$

where the positive and negative torque slopes equations are given by equations (8). The dominant factor affecting the positive $\left(\frac{dT_e^+}{dt}\right)$ and negative $\left(\frac{dT_e^-}{dt}\right)$ slopes is the rotor speed; ω_r . In general, the magnitude of the slopes, are given in Table II.

Table.2. Variation of magnitude of torque slopes with speed

	$\left(\frac{dT_e^+}{dt}\right)$	$\left(\frac{dT_e^-}{dt}\right)$
Low speed	High	Low
Medium speed	Medium	Medium
High speed	Low	High

$$\frac{dT_e^+}{dt} = -T_e \left\{ \frac{1}{\sigma \tau_s} + \frac{1}{\sigma \tau_r} \right\} + \frac{3}{2} \frac{p}{\sigma L_s L_r} \frac{L_m}{L_r} (\vartheta_s - j\omega_r \varphi_s) j\varphi_r$$

$$\frac{dT_e^-}{dt} = -T_e \left\{ \frac{1}{\sigma \tau_s} + \frac{1}{\sigma \tau_r} \right\} - \frac{3}{2} \frac{p}{\sigma L_s L_r} \frac{L_m}{L_r} (j\omega_r \varphi_s) j\varphi_r$$

Note that if $i_s R_s$ is neglected (i.e if $i_s R_s = 0$), condition (7) is always true and hence stator flux can be regulated at all time. Since $v_s - i_s R_s > i_s R_s$ is true for most of the time, for medium and high speed regions, according to Table II, the ratio between the magnitudes of negative torque slope and positive torque slope equals unity or larger than unity, thus condition given by (7) is fulfilled completely. However at low speed region, the problem of stator flux regulation may occur. This problem happens when

$$\frac{\langle \text{negative } T \text{ slope} \rangle}{\langle \text{positive } T \text{ slope} \rangle} \leq \frac{|i_s R_s|}{|(v_s - i_s R_s)|} \tag{8}$$

The flux regulation is determined by the ratio of negative and positive torque slopes as given in equation (8).

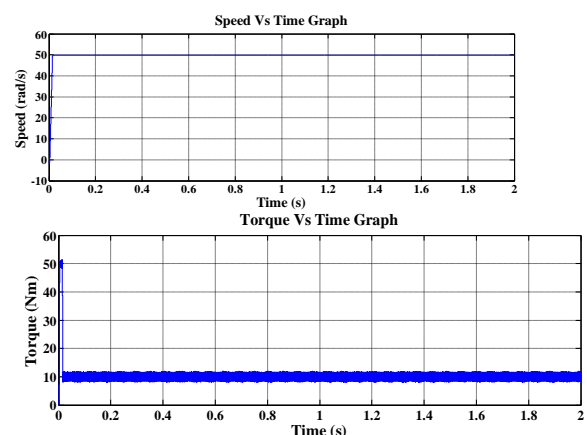


Figure. 3. Results of (a) Speed (b) Torque of DTC-HC.

IV. IMPROVED FLUX REGULATION USING DTC-CSFC AT LOW SPEED

The Hysteresis controller produces variable switching frequency and produce large torque ripples. So, various methods have been proposed to overcome these disadvantages including the use of variable hysteresis bands, predictive control schemes, space vector modulation. DTC is a simple control structure.

Here a new torque controller [12], which produces torque with constant switching frequency and has very low ripple, has been presented.

Here we replace the conventional hysteresis comparator (HC) with a fixed switching frequency controller. The switching frequency is independent of the operating conditions and equals the triangular waveform frequency. A fixed switching frequency is obtained by comparing the triangular waveforms given with the compensated error signals.

That is, the switching frequency is limited by the sampling period of the processor.

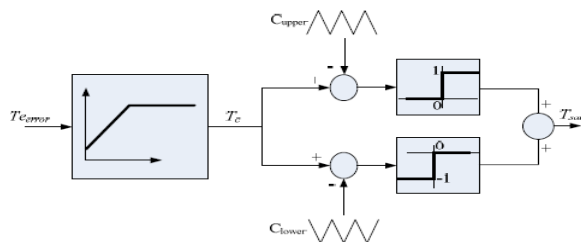


Figure 5. Constant Switching Frequency Controller

By replacing the hysteresis controller (HC) with a modified controller which has a constant switching frequency. As shown in the Fig. 5, the modified torque controller consists of two triangular waveform generators, two comparators and a PI controller.

The two triangular waveforms (C_{upper} and C_{lower}) are 180° out of phase with each other. The carrier wave and system has the same frequency. The absolute values of the DC offsets for the triangular waveforms are set to half of its peak-peak values.

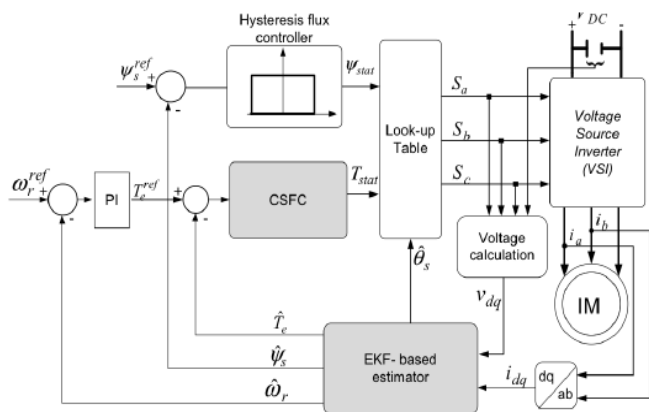


Figure 6. Proposed EKF based DTC-CSFC.

The instantaneous output of the modified torque controller, $q_1(t)$ and the three-level hysteresis comparator used in the conventional DTC, that can be one of the three states: -1, 0 or 1 with the following conditions.

$$T_c = \begin{cases} 1 & \text{for } T_c \geq C_{upper} \\ 0 & \text{for } C_{lower} < T_c < C_{upper} \\ -1 & \text{for } T_c \leq C_{lower} \end{cases} \quad (9)$$

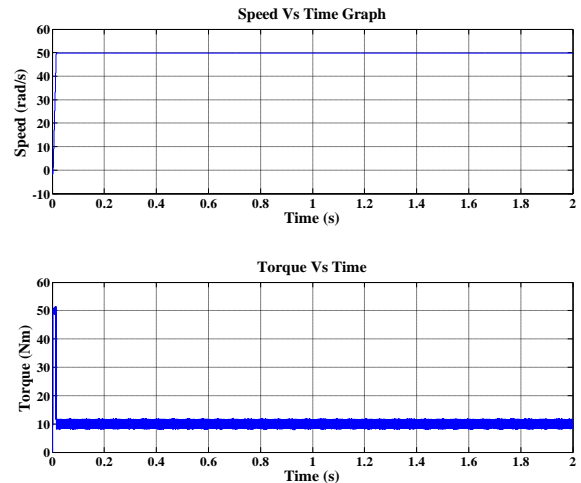


Figure 7. Results of (a) Speed (b) Torque of DTC-CSFC

V. EKF ALGORITHM

There are many speed vector control methods. The system may be under the influence of two types of noises: process noise and system noise. An Extended Kalman Filter is an optimum state-observer that can be used for the state and parameter estimation of a non-linear dynamic system in real time by using noisy signals that are distributed by random noise and assumes that the measurement noise and system noise are uncorrelated. The Extended Kalman Filter (EKF) is used for the estimation of the rotor speed, torque and flux of an induction motor. The EKF is suitable for using in high-performance induction motor drives, and it can provide accurate speed-estimates in a wide speed range and even in very low speeds as well. It is important that the rotor speed has been considered as a state variable and the system matrix A is non-linear and it contains the speed, $A=A(x)$. Thus,

$$\frac{dx}{dt} = Ax + Bu \quad (11)$$

$$y = Cx \quad (12)$$

$$A = \begin{bmatrix} -\frac{K_r}{K_1} & 0 & \frac{L_m R_r}{L_r^2 K_1} & -\frac{L_m \omega_r}{L_r K_l} & 0 \\ 0 & -\frac{K_r}{K_1} & -\frac{L_m \omega_r}{L_r K_l} & \frac{L_m R_r}{L_r^2 K_1} & 0 \\ -\frac{L_m}{T_r} & 0 & -\frac{1}{T_r} & -\omega_r & 0 \\ 0 & \frac{L_m}{T_r} & \omega_r & -\frac{1}{T_r} & 0 \\ 0 & 0 & 0 & 0 & 0 \end{bmatrix}$$

$$B = \begin{bmatrix} 1 & 0 \\ 0 & 1 \\ 0 & 0 \\ 0 & 0 \\ 0 & 0 \end{bmatrix}$$

$$C = \begin{bmatrix} 1 & 0 & 0 & 0 & 0 \\ 0 & 1 & 0 & 0 & 0 \end{bmatrix}$$

$$x = [i_{ds} \quad i_{qs} \quad \Psi_{dr} \quad \Psi_{qr} \quad \omega_r]^T$$

x is the state vector and u is the input vector, A is the system matrix and C is the output matrix.

$$u = [V_{ds} \quad V_{qs}]$$

The system noise covariance matrix (Q) is a [5x5] matrix, and the measurement noise covariance matrix (R) is a [2x2] matrix. However, by assuming that the noise signals are not correlated, both Q and R are diagonal matrices, and only 5 elements need to be known in Q and 2 elements in R . We assume that the first 2 elements of the diagonal are equal ($q_{11}=q_{22}$), the third and fourth elements in the diagonal of Q are equal ($q_{33}=q_{44}$), so $Q=\text{diag}(q_{11}, q_{11}, q_{33}, q_{33}, q_{55})$ contains only 3 elements which need to be known. Similarly, the two diagonal elements in R are equal ($r_{11}=r_{22}$), thus $R=\text{diag}(r_{11}, r_{11})$. i.e., in total, only 4 noise covariance elements needs to be known.

$$Q = \begin{bmatrix} 3.073 \times 10^{-16} & 0 & 0 & 0 & 0 \\ 0 & 3.073 \times 10^{-16} & 0 & 0 & 0 \\ 0 & 0 & 1.919 \times 10^{-11} & 0 & 0 \\ 0 & 0 & 0 & 1.919 \times 10^{-11} & 0 \\ 0 & 0 & 0 & 0 & 5.956 \times 10^{-6} \end{bmatrix}$$

$$R = \begin{bmatrix} 3.364 \times 10^{-3} & 0 \\ 0 & 3.364 \times 10^{-3} \end{bmatrix}$$

$$P = \begin{bmatrix} 1 & 0 & 0 & 0 & 0 \\ 0 & 1 & 0 & 0 & 0 \\ 0 & 0 & 1 & 0 & 0 \\ 0 & 0 & 0 & 1 & 0 \\ 0 & 0 & 0 & 0 & 1 \end{bmatrix}$$

The EKF equations are obtained by using these formulas:

$$\hat{x}_{k+1/k} = A_k x_{k/k} + B_k u_k \quad (3.13)$$

$$P_{k+1/k} = F_k P_{k/k} F_k^T + Q \quad (3.14)$$

Kalman Gain K ;

$$K_{k+1} = H P_{k+1/k} (H P_{k+1/k} H^T + R)^{-1} \quad (3.15)$$

$$\hat{x}_{k+1/k+1} = \hat{x}_{k+1/k} + K_{k+1} (y_k - H \hat{x}_{k+1/k}) \quad (3.16)$$

Covariance matrix P is given by:

$$P_{k+1/k+1} = (I - K_{k+1} H) P_{k+1/k} \quad (3.17)$$

The EKF algorithm involves two main stages: prediction stage and filtering stage. In the prediction stage, the next predicted states $\hat{x}_{k+1/k}$ and predicted state-error covariance filter,

$P_{k+1/k}$ are processed, while in the filtering stage, $\hat{x}_{k+1/k+1}$ the next estimated states, obtained by calculating the sum of the next predicted states and the correction term. The

correction term, $P_{k+1/k+1}$ is used to obtain the output received from prediction step. Also, the posteriori state error filter is $P_{k+1/k+1}$ calculated. I shown in eqn (17) is the diagonal unity matrix.

The stator flux and torque are obtained from the estimated state variables as follows:

$$\Psi_{sd} = \frac{L_m}{L_r} \Psi_{rd} + K_1 i_{sd}$$

$$\Psi_{sq} = \frac{L_m}{L_r} \Psi_{rq} + K_1 i_{sq}$$

$$T_e = \frac{3}{2} \frac{p}{2} \frac{L_m}{L_r} (i_{sq} \Psi_{dr} - i_{sd} \Psi_{qr})$$

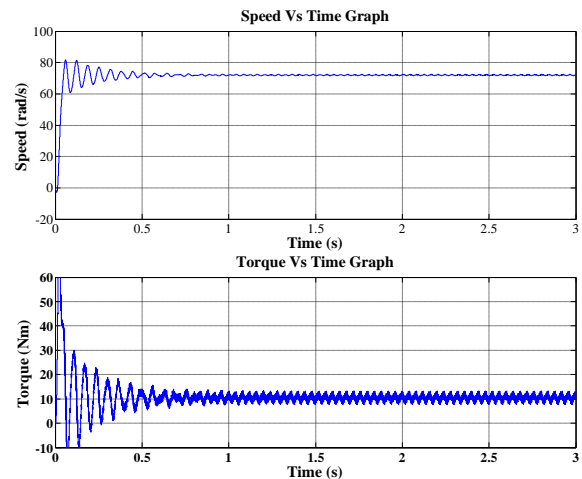


Figure.8. Results of (a) Speed (b) Torque of DTC-EKF.

VI. CONCLUSION

In this paper, the hysteresis torque controller is replaced with CSFC for improving the flux regulation of a lookup table based DTC, so that the state estimations at very low and zero speed operations are also improved. Also the simple structure of DTC-HC is maintained. By using the estimated speed as the feedback, a closed-loop speed control is constructed, to test the performance of the DTC-CSFC. The result shows a significant improvement in flux regulation of DTC-CSFC and thus improving the torque and speed estimations at very low speed operations. Here the normal flux and torque estimator is replaced by EKF estimator. Thus the EKF-based DTC-CSFC reduced the torque ripple at low speed regions.

VII. REFERENCES

- [1].Takahashi and T. Noguchi, "A New Quick-Response and High- Efficiency Control Strategy of an Induction Motor," IEEE Trans. Ind.App., vol. IA-22, pp. 820-827, 1986.
- [2].A. B. Jidin, N. R. B. N. Idris, A. B. M. Yatim, M. E. Elbuluk, and T. Sutikno, "A Wide-Speed High Torque Capability Utilizing Overmodulation Strategy in DTC of Induction Machines With Constant Switching Frequency Controller," Power Electronics, IEEE Transactions on, vol. 27, pp. 2566-2575, 2012.
- [3].Nor Faezah Alias,Auzani Jidin, Mohd Azmi Said, Abdul Rahim Abdulla, "Improved Performance of Direct Torque Control of Induction Machine with 3-Level Neutral Point

Clamped Multilevel Inverter” Electrical machines and system, vol. 26

[4].I. M. Alsofyani and N. R. N. Idris, "A review on sensorless techniques for sustainable reliability and efficient variable frequency drives of induction motors," J. Renewable and Sustainable Energy Reviews, vol. 24, pp. 111-121, 2013.

[5].N. R. N. Idris and A. H. M. Yatim, "Direct torque control of induction machines with constant switching frequency and reduced torque ripple," IEEE Trans. Ind. Electron., vol. 51, pp. 758-767, 2004.

[6].D. Stojić, M. Milinković, S. Veinović, and I. Klasnić, "Improved Stator Flux Estimator for Speed Sensorless Induction Motor Drives," IEEE Trans. Power Electronics, vol. 30, pp. 2363-2371, 2015.

[7].D. Stojić, M. Milinković, S. Veinović, and I. Klasnić, "Improved Stator Flux Estimator for Speed Sensorless Induction Motor Drives," IEEE Trans. Power Electronics, vol. 30, pp. 2363-2371, 2015.

[8].W.S.H. Wong and D. Holliday, "Minimisation of flux droop in direct torquecontrolled induction motor drives," Electric Power Applications, vol. 151, pp. 694 - 703, 2004.

[9].L. Kyo-Beum, S. Joong-Ho, I. Choy, and Y. Ji-Yoon, "Improvement of low-speed operation performance of DTC for three-level inverterfed induction motors," IEEE Trans. Ind. Electronics, vol. 48, pp. 1006-1014, 2001.

[10].S. Kuo-Kai, S. Li-Jen, C. Hwang-Zhi, and J. Ko-Wen, "Flux compensated direct torque control of induction motor drives for low speed operation," IEEE Trans. Power Electronics, vol. 19, pp. 1608- 1613, 2004.

[11].I. M. Alsofyani, N. R. N. Idris, Y. A. Alamri, S. A. Anbaran, A. Wangsuphaphol, and W. Y. Low, "Improved EKF-based direct torque control at the start-up using constant switching frequency," in Proc. IEEE Energy Conversion Conf., 2014, pp. 237-242.

[12].B. K. Bose, "An adaptive hysteresis-band current control technique for a voltage-fed PWM inverter for machine drive system," IEEE Trans. Ind. Electron., vol. 37, no. 5, pp. 402–408, Oct. 1990.

[13].N. R. N. Idris, A. H. M. Yatim, (2000) "Reduced torque ripple and constant torque switching frequency strategy for Direct Torque Control of induction machine", 15th IEEE-Applied Power Electronics Conference and Exhibition 2000 (APEC 2000), Vol. 1, pp. 154-161.